ACS Macro Letters

Letter

pubs.acs.org/macroletters

Self-Assembly of Hybridized Peptide Nucleic Acid Amphiphiles

Li-Han Liu, Ze-Yong Li, Lei Rong, Si-Yong Qin, Qi Lei, Han Cheng, Xiang Zhou, Ren-Xi Zhuo, and Xian-Zheng Zhang*

Key Laboratory of Biomedical Polymers of Ministry of Education and Department of Chemistry, Wuhan University, Wuhan 430072, China

Supporting Information

ABSTRACT: In this report, a series of peptide nucleic acid amphiphiles (PNAAs) with hybridization properties were designed and synthesized. Driven by hydrophobic interaction, the hybridized PNAAs can form uniform micelles, the base stacking interaction from PNA segments further stabilized the micelles. The effects of hydrophobic alkyl chain length, structure of hydrophilic peptides, concentration, and pH on the self-assembly behavior of partly complementing PNAA duplexes were explored.

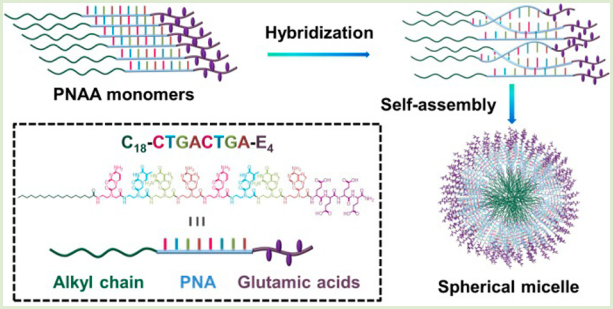

Inspired by the DNA double helix, peptide nucleic acids (PNAs) are designed to hybridize with the complementary sequence (DNA, RNA, or PNA) using the uncharged *N*-(2-aminoethyl)glycine (pseudopeptide) backbone instead of DNA's negatively charged sugar phosphate backbone. Owning to its nonelectrostatic repulsion, PNAs have higher binding affinity and specificity to oligonucleotides than DNA/DNA or RNA/RNA.[1,2] Meanwhile, pseudopeptide backbone also endows PNAs with many other advantages. For example, PNA oligomers can be easily synthesized by standard solid phase peptide synthesis protocols (SPPS). Functional groups can be attached to PNAs through the N-terminal amino group and the C-terminal carboxylic acid group. Moreover, PNAs are chemically stable and resistant to nucleases and proteases.[3] These unique chemical and biological properties of PNAs make them of great importance in producing powerful materials such as biomolecule tools, biosensors, molecular probes, and antigene and antisense agents.[4]

Self-assembly is an attractive method to prepare functional nanomaterial.[5−7] Self-assembly materials created by linking bioactive peptides with lipophilic moieties (named peptide amphiphiles (PA)) have attracted much attention for their promised biomedical applications.[8] Based on the advantages of PNA, it is believed that the combination of the hydrophobic interaction from the structure feature of PA and the multiple hydrogen bonds from the PNA hybridization can be utilized to fabricate novel supermolecules and functional nanomaterials with new potential applications such as bioseparation and biosensing[5] by noncovalent self-assembly. A peptide nucleic acid/peptide amphiphile conjugate (PNA−PA) was reported to self-assemble into nanostructures that could bind oligonucleotides with high affinity and high specificity.[9] Schneider et al. constructed DNA oligomers binding micelles which were formed by a series of peptide nucleic acid amphiphiles.[1] However, this work mainly focuses on the binding property of PNA to DNA and their self-assemble behaviors, but the self-assemble behaviors of PNA to PNA still remain unclear. In this paper, the self-assemble behaviors and the possible assembly mechanism of PNA-amphiphiles with PNA hybridization and amphiphilic properties were investigated.

In this work, a series of PNA-amphiphiles (PNAAs) with different hydrophobic and hydrophilic moieties, that is, C_2-CTGACTGA-E_4 (PNAA1), C_6-CTGACTGA-E_4 (PNAA2), C_{12}-CTGACTGA-E_4 (PNAA3), C_{18}-CTGACTGA-E_4 (PNAA4), and C_{12}-CTGACTGA-E_2 (PNAA5), were designed and synthesized. As shown in Figure 1a, these PNAAs consist of three parts. The first part is the peptide nucleic acid segment with the ability to form a duplex with another PNAA molecule through base pairing. The two other parts are the hydrophilic peptide segment with anionic amino acids (glutamic acid) and hydrophobic alkyl chain segment, which cooperated together to make the whole molecule amphiphilic. PNA sequence CTGACTGA was chosen for its ability to partly hybridize with another same sequence in parallel (see Figure 1b). We supposed that the PNAAs would self-assemble into nanostructure in water with its amphiphilic feature and the stacking interaction between nucleobases. Hybridization of two PNAAs in a parallel pattern formed the gemini-like[10] structured amphiphile, which further self-assembled into micelle. The subtle diversification of PNAA structure was used to demonstrate the influence of the length of alkyl tails and the number of anionic amino acids on the self-assembly behavior of PNAAs.

Received: March 31, 2014
Accepted: May 2, 2014
Published: May 6, 2014

dx.doi.org/10.1021/mz5001916 | *ACS Macro Lett.* 2014, 3, 467−471

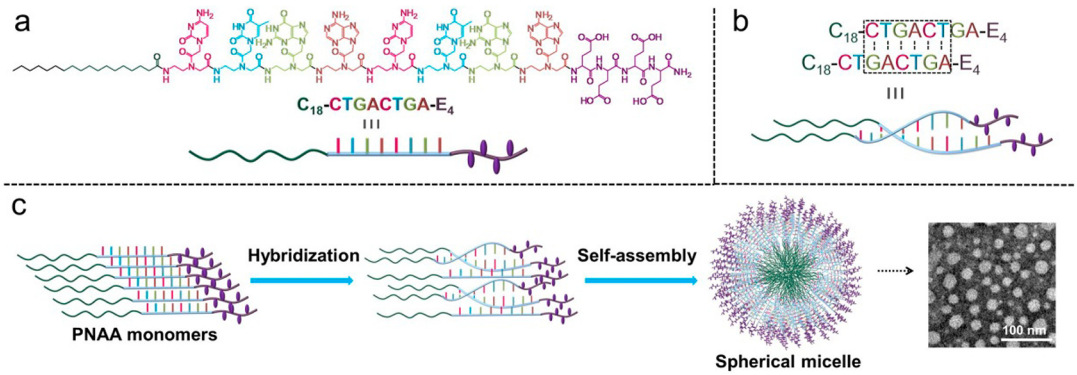

Figure 1. (a) Structure of C_{18}-ctgactga-E_4; (b) Formation of PNAA duplex; (c) Self-assembly of PNAAs, exampled with PNAA4. The structures of PNAA duplexes in this figure do not represent its helicity.

Five PNA-amphiphiles (PNAA1−5) were synthesized manually by solid-phase synthesis using Fmoc/Bhoc protected PNA monomers on the Fmoc protected Rink Amide resin (see Supporting Information).[1,11] In order to study their self-assembly behaviors, PNAA1−5 were dissolved in 10 mM sodium phosphate buffer (pH 7.4). PNAA micelles formation was carried out by the excitation spectrum of fluorescence spectroscopy using hydrophobic pyrene fluorescent probe in the former mentioned buffer.[12] The increase in fluorescence intensity, as well as a red-shift from 337 to 341 nm occurs, indicated the micellization of PNAAs, because pyrene is preferentially diffused into hydrophobic core of PNAA micelles, resulting in a change of its photophysical properties.[12] As shown in Figure 2d−f, PNAA3−5 can self-assemble into micelles at the very low critical micelle concentration (CMC) values by 45.7 μM (0.13 mg mL^{-1}), 6.1 μM (0.016 mg mL^{-1}), and 3.1 μM (0.009 mg mL^{-1}), respectively. It could be noticed that the CMC values of the PNAAs increased with increasing hydrophilic and hydrophobic ratio.[13] These data suggested the high importance of the hydrophilic and hydrophobic interactions for the successful micelle formation. The extremely low CMC of PNAAs is somewhat consistent with the low CMC property of gemini surfactants. However, only 1 nm red-shift was found in the fluorescence spectra of PNAA1 and PNAA2 solution, which indicated that PNAA1 and PNAA2 cannot form regularly shaped micelles at low concentration. It may attributed to their too short alky chains, which result in the unfavorable geometrical effect and weaker hydrophobic interaction.[14] Otherwise, the critical aggregation concentration (CAC) shown the aggregation of PNAA1 and -2 (may not be micelles) when their concentration is higher than 78.3 and 58.5 μM, respectively (Figure S3).

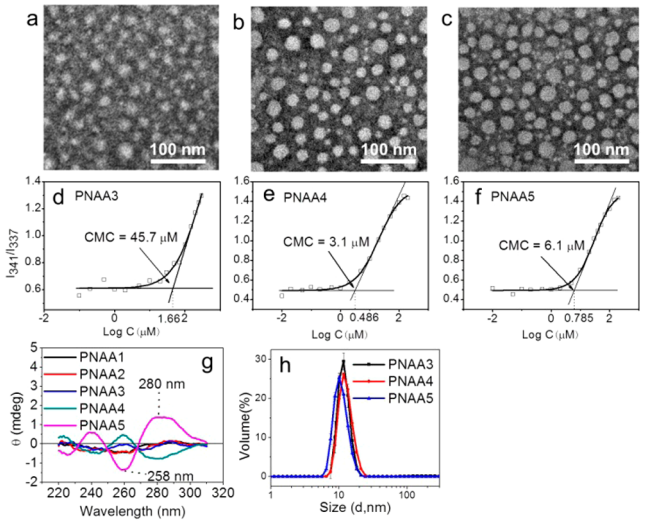

Figure 2. TEM images of self-assembled PNAA3 (a), PNAA4 (b), and PNAA5 (c) at a concentration of 300, 100, and 100 μM, respectively. The intensity ratio I_{341}/I_{337} was plotted as a function of logarithm of PNAA concentrations (e−g) and the calculated CMC value. CD spectra of the self-assembled PNAAs micelles solutions (g) in which all PNAAs are at the concentration of 100 μM. Size distribution of the PNAA3, PNAA4, and PNAA5 micelles at 300, 100, and 100 μM investigated by volume (h).

To further investigate the influence of the hydrophilic and hydrophobic interactions on the formed micelles, the size distribution and morphology of the self-assembled PNAAs micelles in the former mentioned buffer were studied by dynamic light scattering (DLS) and transmission electron microscopy (TEM). As shown in Figure 2a−c, PNAA3−5 can self-assemble into well-defined spherical micelles with diameter of about 5−30 nm, which was approximate to the DLS value (see Figure 2h). The discrepancy between the DLS and TEM consequences was mainly ascribed to the different measuring methods. For the preparation of TEM sample, PNAAs may aggregate during the air-drying process, resulting in larger particles due to partial aggregation of original micelles. These results indicated that the subtle diversification of PNAA structure (various lengths of hydrophobic alkyne chain or anionic amino acid segments) did not have much influence on the micelle size.

The second structure of the forming micelles at the same concentration (100 μM) in aqueous solution was also investigated by circular dichroism (CD) spectroscopy. First, the handedness of PNAA duplexes was studied at low concentration by adding $DiSC_2(5)$ dye to diluted PNAA solution according to the method reported by Armitage et al.[15] It was reported that symmetrical cyanine dyes containing benzothiazole groups bind to a variety of PNA-containing hybrids, including PNA/DNA duplexes, PNA/PNA duplexes with high affinity. The CD spectra of PNAA solutions containing DiSC2(5) (Figure S4) at low concentration were recorded, and it was found that all of the five PNAAs duplexes are left-handed.[16,17] However, different CD signals were observed at higher concentration (far more above the CMC) at the wavelength from 220 to 300 nm. As shown in Figure 2g, the characteristic negative band at 258 nm and positive band at

dx.doi.org/10.1021/mz5001916 | ACS Macro Lett. 2014, 3, 467−471

280 nm (Figure 2g, magenta line) indicated that the handedness of self-assembled PNAA5 micelle structure might be left handed from the evidence observed from previous report.[15−17] Weak right-handed helix could be found in the self-assembled micelles of PNAA4 (Figure 2g, dark cyan line). There is almost no significant CD structure corresponded to asymmetrical double helix of oligonucleotides in PNAA1−3 (Figure 2g, black, red, and blue line). By comparing the different CD spectra of PNAA3 (Figure S5, magenta line) with PNAA5 (Figure 2g, magenta line), it was also found that PNAA duplexes with the same alkyl chain, but different numbers of glutamic acid residues, would result in different CD signals at higher concentrations. These different CD signals may be ascribed to the disparity of the PNAA primary structure, which would result in different second structures as the further compact packing of base pairs, stronger electrostatic repulsion occurred between terminal carboxyl groups, and stronger interactions existed on residues and PNA base pairs in micelles.

The influence of PNAA concentration on the second structure of PNAA micelles was also investigated. As shown in Figure 3b and Figure S4, the secondary structure of self-assembled micelles changes with the increase of micelle concentration. For PNAA5, there were no significant CD signal at 20 μM, but shown increased characteristic negative band at 258 nm and positive band at 280 nm as the concentration increased from 50 to 200 μM. Also, PNAA3 only have significant CD signal in 220 to 320 nm at the high concentration (300 μM; Figure S4). Changed CD signals indicated the changed stacking form of bases in the PNAA micelles at high concentrations. The curves indicated that PNAAs formed loose stacking assemblies at low concentrations near the CMC value, which have no CD signals at 220 to 320 nm, but at higher concentrations, significant CD peaks were shown owing to the compact stacking of PNAAs and stronger interactions inside micelle such as stronger base stacking interaction between adjacent PNAAs.

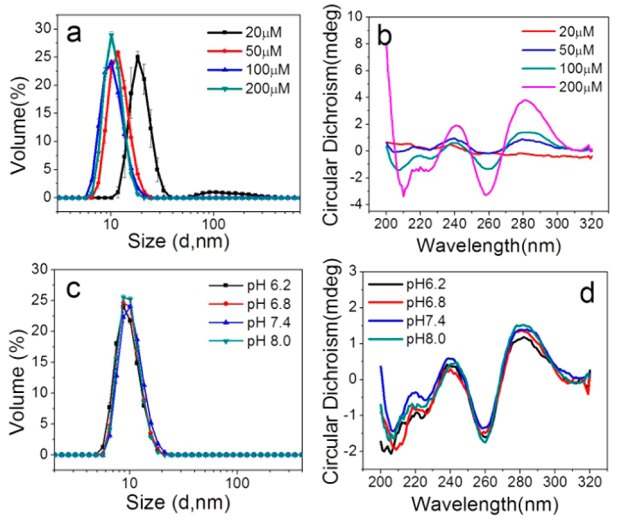

Figure 3. Size distribution of the PNAA5 micelles investigated by volume (a) and CD spectra of the self-assembled PNAA5 micelles (b) at a concentration of 20, 50, 100, and 200 μM. The size distribution of the PNAA5 micelles investigated by volume (c) and CD spectra of the self-assembled PNAA5 micelles (d) at a concentration of 100 μM in 10 mM sodium phosphate buffer (pH 6.2, 6.8, 7.4, and 8.0).

The influence of PNAA concentration on the size of PNAA micelles was studied following. Size distribution of self-assembled PNAA5 micelles was detected at several concentrations. As shown in Figure 3a, the size of PNAA aggregates changed as the increased concentration, there were one peak at about 10 nm at 50, 100, and 200 μM, but two peaks at the concentration near the CMC value (20 μM), which may result from the loose stacking of PNAA self-assembly segments at low concentration, but at higher concentrations, PNAAs formed tight assemblies with relatively smaller size.

Since the carboxylic group at the side chains of glutamic acid have a pK_a of about 4.1, it will be almost deprotonated at the neutral pH.[18−20] Therefore, at around neutral pH, the self-assembly of PNAAs would show little pH dependence, which was demonstrated by CD spectra and DLS analyses. For example, as shown in Figure 3c,d, CD signal and the size distribution of PNAA5 is extremely similar at various pHs ranging from 6.2 to 8.0.

The formation of PNAA duplexes was further demonstrated by observing the color change induced by PNAAs' interaction with cyanine dye. Upon binding to PNA/PNA duplexes, 3, 3′-diethylthiadicarbocyanine dye $DiSC_2(5)$ change its color from blue to purple.[21] As shown in Figure 4a, all of the five $DiSC_2(5)$ solutions containing PNAA were purple, while the control remains blue. UV−vis absorbance was further recorded (Figure 4b) and it was found the addition of PNAA caused a dramatic change in the spectra, that is, the new absorption at 539 nm appeared, corresponding to the specific absorption of the PNAA bound cyanine. This indicated that PNAA hybrids existed at the concentration of 10 μM, which is much lower than its CMC, suggesting that PNAAs might form hybrids before the formation of micelles. Noteworthy, encapsulation of $DiSC_2(5)$ within the hydrophobic core cannot induce a new absorption band at around 540 nm (Figure S6). Melting temperature of PNAA3 (26.1 °C) based on UV melting curves, also implied the formation of PNA Wat son-Crick duplexes at 10 μM (Figure S7). Verification experiment of concentration dependence in UV−vis absorbance of PNAA with $DiSC_2(5)$ was further carried out (Figure S8). The increased absorbance at 539 nm indicated the number of PNAA hybrids was

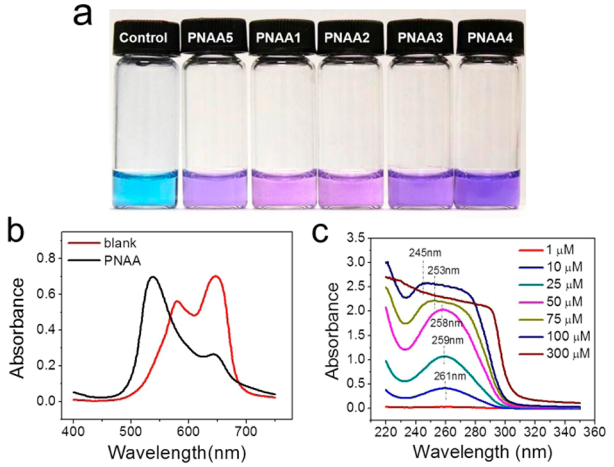

Figure 4. (a) PNAAs hybridization of PNAA (10 μM) in $DiSC_2(5)$ (15 μM) inducing a blue to purple color change (The $DiSC_2(5)$ (15 μM) was used as a control). (b) UV−vis spectrum of $DiSC_2(5)$ (15 μM) (blank) and $DiSC_2(5)$ containing PNAA 3 (10 μM). (c) UV−vis spectrum of PNAA3 at different concentrations.

dx.doi.org/10.1021/mz5001916 | ACS Macro Lett. 2014, 3, 467−471

increased with the increasing PNAA5 concentration, even when PNAA5 began to form micelles. This observation suggested that PNAAs could form hybrids before the formation of micelles, and the hybrids also existed in micelles.

In this study, UV−vis spectrum was employed to verify the base stacking interaction existed in the self-assembled PNAA micelles. UV spectra of nucleic acids are sensitive to conformation changes, because stacking of the nucleotide bases in helical structures would lead to hypochromicity at around 260 nm.[22] Since there are four natural nucleobases in PNA backbone, it is believed that phenomenon of hypochromicity of PNAA at 260 nm was responsible to the stacking of the nucleobases in PNAA micelles. The self-assembled PNAA3 in sodium phosphate buffer (10 mM, pH 7.4) with different concentration (1−300 μM) were prepared for UV−vis analysis. As shown in Figure 4c, the absorption in 260 nm was increased coincided with the increasing micelle concentration at 1 μM to 50 μM but slowly at 50 μM to 100 μM, and the absorption in 260 nm at 300 μM was even lower than 100 μM. Meanwhile, the maximum absorption peak of the UV spectrum shifted from 261 to 245 nm when the concentration increased from 1 to 100 μM, and no peak at 300 μM. The visibly hypochromicity phenomenon at 260 nm demonstrated that PNAAs duplexes began to form aggregates and resulted in more compact base stacking when the concentration was as high as 50 μM, which was coincided with the CMC consequence.

Based on above results, the probable self-assembly mechanism of PNAAs was proposed as shown in Figure 1. The rationally designed hybridized PNAAs perform the ability to form well-defined spherical micelles via hydrophobic interaction which make alkyl chains stack together in the micellar core,[23,24] and the base stacking interaction from PNA segments further stabilized the micelles. Meanwhile, the hydrophilic interaction provided by negative charged amino acids residues[5] in the shell make the micelles stable in 10 mM sodium phosphate buffer (pH 7.4). The presence of different residues within the PNA terminal would result in different self-assembly behavior and different second structures but the same morphology. Different from shell cross-linked micelles in which the shell of micelles was cross-linked via some certain reactions, the obtained micelles were attributed to the molecular self-assembly of PNAAs. Herein, due to the presence of peptide nucleic acids segments, these micelles may be applied as nanosensor for biomedical detection such as examining the presence of several kinds of oligonucleotides with specific sequence since peptide nucleic acids have been reported to be used to the SNP detection[21,25] and DNA detection.[26,27] Moreover, these micelles are promised to be applied to sequence-specific oligonucleotide purification,[28] inhibition of gene expression,[1] and gene delivery.[29]

In summary, rationally designed complementary structured peptide nucleic acid amphiphiles (PNAA1−5) were successfully synthesized. Due to the base pair stacking of PNAA duplexes and proper intermolecular hydrophobic/hydrophilic interaction, PNAA3−5 can spontaneously self-assemble into well-defined spherical micelles in sodium phosphate buffer (10 mM, pH 7.4) with different secondary structures. These self-assembled peptide nucleic acid amphiphiles based micelles would find great potential in biomedical applications such as oligonucleotide purification, gene inhibitors, and biosensors.

■ ASSOCIATED CONTENT

Supporting Information

Experiment details and supplemental figures. This material is available free of charge via the Internet at http://pubs.acs.org.

■ AUTHOR INFORMATION

Corresponding Author

*Tel. and Fax: 86-27-68754509. E-mail: xz-zhang@whu.edu.cn.

Notes

The authors declare no competing financial interest.

■ ACKNOWLEDGMENTS

This work was supported by National Natural Science Foundation of China (51233003, 51125014), National Key Basic Research Program of China (2011CB606202), and the Ministry of Education of China (20120141130003).

■ REFERENCES

(1) Vernille, J. P.; Kovell, L. C.; Schneider, J. W. *Bioconjugate Chem.* **2004**, *15*, 1314−1321.
(2) Egholm, M.; Buchardt, O.; Christensen, L.; Behrens, C.; Freier, S. M.; Driver, D. A.; Berg, R. H.; Kim, S. K.; Nordén, B.; Nielsen, P. E. *Nature* **1993**, *365*, 566−568.
(3) Hyrup, B.; Nielsen, P. E. *Bioorg. Med. Chem.* **1996**, *4*, 5−23.
(4) Nielsen, P. E.; Egholm, M. *Curr. Issues Mol. Biol.* **1999**, *2*, 89−104.
(5) Lau, C.; Bitton, R.; Peled, H. B.; Schultz, D. G.; Cookson, D. J.; Grosser, S. T.; Schneider, J. W. *J. Phys. Chem. B* **2006**, *110*, 9027−9033.
(6) Xu, J.; Luo, S. Z.; Shi, W. F.; Liu, S. Y. *Langmuir* **2006**, *22*, 989−997.
(7) Ge, Z. S.; Hu, J. M.; Huang, F. H.; Liu, S. Y. *Angew. Chem., Int. Ed.* **2009**, *48*, 1798−1802.
(8) Cui, H. G.; Webber, M. J.; Stupp, S. I. *Pept. Sci.* **2010**, *94*, 1−18.
(9) Guler, M. O.; Pokorski, J. K.; Appella, D. H.; Stupp, S. I. *Bioconjugate Chem.* **2005**, *16*, 501−503.
(10) Menger, F. M.; Littau, C. A. *J. Am. Chem. Soc.* **1991**, *113*, 1451−1452.
(11) Beck, F. Solid Phase Synthesis of PNA Oligomers. In *Peptide Nucleic Acids: Methods and Protocols*; Nielsen, P. E., Ed.; Series: Methods in Molecular Biology; Humana Press Inc.: Totowa, NJ, 2002, Vol. *208*, p 29.
(12) Li, Z. Y.; Wang, H. Y.; Li, C.; Zhang, X. L.; Wu, X. J.; Qin, S. Y.; Zhang, X. Z.; Zhuo, R. X. *J. Polym. Sci., Polym. Chem.* **2011**, *49*, 286−292.
(13) Xu, H.; Wang, J.; Han, S.; Wang, J.; Yu, D.; Zhang, H.; Xia, D.; Zhao, X.; Waigh, T. A.; Lu, J. R. *Langmuir* **2009**, *25*, 4115−4123.
(14) Hartgerink, J. D.; Beniash, E.; Stupp, S. I. *Proc. Natl. Acad. Sci. U.S.A.* **2002**, *99*, 5133−5138.
(15) Smith, J. O.; Olson, D. A.; Armitage, B. A. *J. Am. Chem. Soc.* **1999**, *121*, 2686−2695.
(16) Lagriffoule, P.; Wittung, P.; Erikkson, M.; Jensen, K. K.; Nordén, B.; Buchardt, O.; Nielsen, P. E. *Chem.—Eur. J.* **1997**, *3*, 912−919.
(17) Tedeschi, T.; Sforza, S.; Dossena, A.; Corradini, R.; Marchelli, R. *Chirality* **2005**, *17*, 196−204.
(18) Santos, D. P.; Zanoni, M. V. B.; Bergamini, M. F.; Chiorcea-Paquim, A. M.; Diculescu, V. C.; Brett, A. M. O. *Electrochim. Acta* **2008**, *53*, 3991−4000.
(19) Stephen Inbaraj, B.; Wang, J. S.; Lu, J. F.; Siao, F. Y.; Chen, B. H. *Bioresour. Technol.* **2009**, *100*, 200−207.
(20) Rao, J. Y.; Zhang, Y. F.; Zhang, J. Y.; Liu, S. Y. *Biomacromolecules* **2008**, *9*, 2586−2593.
(21) Komiyama, M.; Sheng, Y.; Liang, X. G.; Yamamoto, Y.; Tomita, T.; Zhou, J. M.; Aburatani, H. *J. Am. Chem. Soc.* **2003**, *125*, 3758−3762.

(22) Cooper, A. *Biophysical Chemistry*; The Royal Society of Chemistry: Cambridge, 2004; Chapter 2, p 28.
(23) Nagarajan, R.; Ganesh, K. *J. Chem. Phys.* **1989**, *90*, 5843−5856.
(24) Hartgerink, J. D.; Beniash, E.; Stupp, S. I. *Science* **2001**, *294*, 1684−1688.
(25) Gaylord, B. S.; Massie, M. R.; Feinstein, S. C.; Baza, G. C. *Proc. Natl. Acad. Sci. U.S.A.* **2005**, *10*, 34−39.
(26) Fabris, L.; Dante, M.; Braun, G.; Lee, S. J.; Reich, N. O.; Moskovits, M.; Nguyen, T. Q.; Bazan, G. C. *J. Am. Chem. Soc.* **2007**, *129*, 6086−6087.
(27) Tian, K.; He, Z. j.; Wang, Y.; Chen, S. J.; Gu, L. Q. *ACS Nano* **2013**, *7*, 3962−3969.
(28) Vernille, J. P.; Schneider, J. W. *Biotechnol. Prog.* **2004**, *20*, 1776−1782.
(29) Liang, K. W.; Hoffman, E. P.; Huang, L. *Mol. Ther.* **2000**, *1*, 236−243.